Sesquiterpenoids from *Dysoxylum acutangulum* Miq. Twigs and Their Antibiofilm Activity Against *Streptococcus mutans*

Risyandi Anwar *, Hikma Ainazzahra, Citra Nisa Ul Inayah, Al Arofatus Naini, Endang Juliansyah, Elpri Eka Permadi, Aditya Nugroho, Kindi Farabi, Unang Supratman *

Posted Date: 31 March 2026

doi: 10.20944/preprints202603.2471.v1

Keywords: sesquiterpenoids; *Dysoxylum acutangulum*; antibiofilm; *Streptococcus mutans*

 doi:10.20944/preprints202603.2471.v1

Article

Sesquiterpenoids from *Dysoxylum acutangulum* Miq. Twigs and Their Antibiofilm Activity Against *Streptococcus mutans*

Risyandi Anwar [1,*], Hikma Ainazzahra [2], Citra Nisa Ul Inayah [2], Al Arofatus Naini [3], Endang Juliansyah [2], Elpri Eka Permadi [3], Aditya Nugroho [4], Kindi Farabi [2] and Unang Supratman [2,5]

[1] Herbal Medicine Research, Department of Pediatric Dentistry, Faculty of Dental Medicine, University of Muhammadiyah Semarang, Semarang 50272, Indonesia
[2] Department of Chemistry, Faculty of Mathematics and Natural Sciences, Universitas Padjadjaran, Jl. Raya Bandung–Sumedang Km. 21, Jatinangor, Sumedang 45363, Indonesia
[3] Research Center for Pharmaceutical Ingredients and Traditional Medicine, National Research and Innovation Agency (BRIN), Cibinong Science Center Complex – BRIN, Cibinong 16911, Bogor, West Java, Indonesia
[4] Research Center for Applied Botany, National Research and Innovation Agency (BRIN), Cibinong Science Center Complex – BRIN, Cibinong 16911, Bogor, West Java, Indonesia
[5] Central Laboratory, Universitas Padjadjaran, Jl. Raya Bandung–Sumedang Km. 21, Jatinangor, Sumedang 45363, Indonesia
* Correspondence: drg.risyandi@unimus.ac.id; Tel.: +62-24-76740293

Abstract

Sesquiterpenoids are terpenoid-derived compounds with diverse biological activities and are commonly found in plants of the *Dysoxylum* genus (Meliaceae). This study aimed to isolate and characterize sesquiterpenoids from the *n*-hexane extract of *Dysoxylum acutangulum* Miq. and to evaluate their antibiofilm activity against *Streptococcus mutans*. The extract was separated using various chromatographic techniques to yield one tricyclic sesquiterpenoid and one mixture of epimeric sesquiterpenoids. Structural elucidation was performed using spectroscopic analyses, including MS, IR, and NMR, and by comparison with reported data. The isolated compounds were identified as spathulenol (**1**), 10-oxo-isodauc-3-en-15-al (**2a**, mayor), and sinulin A (**2b**, minor). In vitro testing showed weak antibiofilm activity (MBIC 250–500 μg/mL) and no significant inhibition at 62.5 μg/mL compared to chlorhexidine. Molecular docking against Sortase A and GtfB revealed moderate binding affinities consistent with the experimental trend. The slightly better activity of the epimeric mixture suggests a possible additive effect. Overall, these findings provide preliminary structure–activity insights into sesquiterpenoids from *D. acutangulum* as potential antibiofilm candidates, warranting further mechanistic and combination-based investigations.

Keywords: sesquiterpenoids; *Dysoxylum acutangulum*; antibiofilm; *Streptococcus mutans*

1. Introduction

Sesquiterpenoids are the most abundant class of terpenoids, biosynthetically derived from three isoprene units. As of 2014, more than 10,000 sesquiterpenoids with diverse and structurally intriguing scaffolds had been reported [1]. These compounds play essential roles in various sectors, particularly as major constituents of fragrances along with monoterpenoids [2,3]. In recent years, sesquiterpenoids have also attracted considerable attention due to their broad range of pharmacological activities, including neuroprotective, anti-inflammatory, antidepressant, anti-hepatic fibrosis, and antibacterial effects [4–7]. Notably, several newly identified sesquiterpenoids

 doi:10.20944/preprints202603.2471.v1

from natural sources have demonstrated significant antibacterial activity against pathogenic bacteria such as Staphylococcus aureus, methicillin-resistant Staphylococcus aureus (MRSA), Bacillus spp., Erwinia carotovora, and Pseudomonas spp. [8,9].

The discovery of antibacterial sesquiterpenoids has further encouraged research in more targeted areas, particularly antibiofilm activity. Biofilms are structured communities of microorganisms that adhere to surfaces and grow as collective entities. They are estimated to be responsible for approximately 65–80% of chronic infections in the human body and have been detected in nearly all organ systems, including the digestive and excretory systems. Biofilm-associated diseases include acute pneumonia, chronic rhinosinusitis, chronic otitis media, urinary tract infections, chronic prostatitis, bacterial vaginosis, osteomyelitis, atherosclerosis, dental caries, gastric ulcers, and inflammatory bowel disease [10,11]. Both Gram-positive and Gram-negative bacteria are capable of forming biofilms; however, *Streptococcus mutans* is among the most prevalent and clinically relevant biofilm-forming bacteria. *S. mutans* plays a central role in the initiation and progression of dental caries through its strong adhesion to tooth surfaces, acidogenic and aciduric properties, and its ability to synthesize extracellular polysaccharides that stabilize biofilm architecture [12]. Consequently, inhibition of *S. mutans* biofilm formation is considered a key strategy for the prevention and management of dental caries, a disease with a reported global prevalence of up to 82.8% [13].

The Meliaceae family, a member of the order Sapindales, comprises tropical plant species that are widely recognized for their valuable timber and fragrant stems. It includes approximately 58 genera with around 740 species [14]. Sesquiterpenoids have been reported from several genera within this family, including *Aglaia* [15], *Dysoxylum* [16], *Chisocheton* [17], *Guarea* [18], *Trichilia* [19], and *Lansium* [20]. The genus *Dysoxylum* exhibits a broad geographical distribution, mainly across tropical and subtropical areas such as China, India, Malaysia, northeastern Australia, and other regions of Southeast Asia. To date, about 200 species of *Dysoxylum* have been identified as sources of diverse secondary metabolites, including sesquiterpenoids [21,22], sesquiterpenoid dimers [23], diterpenoids [24,25], triterpenoids [26–29], limonoids [30–33], and macrolides [34].

Previous studies reported the isolation of phenolic sesquiterpenoids, including dioxophenol and (7*R*,10*S*)-2-hydroxycalamenene, from the twigs of *D. densiflorum*, both of which exhibited antibacterial activity against *Bacillus subtilis* with minimum inhibitory concentration (MIC) values of 28 μM [35]. Motivated by these findings, we investigated the sesquiterpenoid constituents of the less-studied species *D. acutangulum* Miq.. In this study, four sesquiterpenoids representing diverse scaffolds were isolated: spathulenol (**1**), and an isodaucane-type sesquiterpenoid obtained as an epimeric mixture (**2a** and **2b**). Their isolation, structural elucidation, along with in vitro and in silico antibiofilm activities against *S. mutans* are reported herein.

2. Results and Discussion

The ethanolic extract from the twigs of *D. acutangulum* Miq. was macerated and extracted consecutively with *n*-hexane, ethyl acetate, and *n*-butanol. The *n*-hexane extract of *D. acutangulum* was separated by a combination of normal-phase and reversed-phase column chromatography to give compounds **1** and **2**.

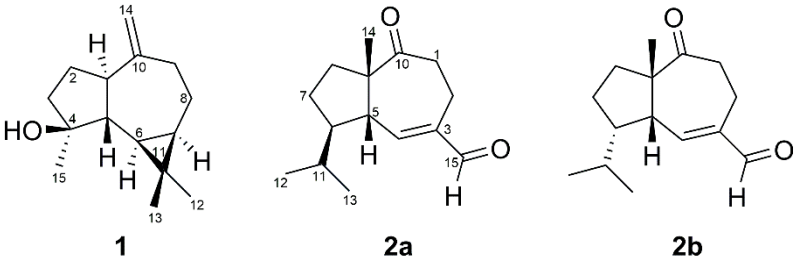

Figure 1. The structure of compounds **1** and **2**.

 doi:10.20944/preprints202603.2471.v1

Compound **1** was isolated as a colorless oil, with a molecular formula $C_{15}H_{24}O$ based on HR-TOFMS with the positive ion peak m/z 221.1918 $[M + H]^+$ (calcd. 221.1905), resulting in four degrees of unsaturation. IR spectra showed absorption bands indicating the presence of hydroxyl (3379 cm^{-1}), C-H sp^3 aliphatic (2927 cm^{-1}), C=C olefinic (1635 cm^{-1}), *gem*-dimethyl (1455 and 1375 cm^{-1}), and ether group (1095 cm^{-1}). The ^{1}H-NMR spectra showed proton resonance related to three tertiary methyls at δ_H 1.04 (3H, s, CH_3-12), 1.06 (3H, s, CH_3-13), and 1.28 (3H, s, CH_3-15), olefinic methylene at δ_H 4.66 (1H, br.s, H-14) and 4.69 (1H, br.s, H-14), as well as two methines at δ_H 0.46 (1H, dd, *J*=9.5, 11.3 Hz, H-6) and 0.71 (1H, ddd, *J*=11.3, 9.4, 6.1 Hz, H-7). Analysis of ^{13}C-NMR supported by DEPT 135° spectra of compound **1** shows 15 carbons resonance consisting of three methyls at δ_c [16.3 (C-12), 26.1 (C-15), 28.6 (C-13)], one aliphatic quaternary carbon δ_c [20.3 (C-11)], four aliphatic methylenes δ_c [24.8 (C-8), 26.7 (C-2), 38.8 (C-9), 41.7 (C-3)], four aliphatic methylenes δ_c [27.5 (C7), 29.9 (C-6), 53.4 (C-1), 54.3 (C-5)], one oxygenated quaternary carbon δ_c [81.0 (C-4)], one olefinic methylene δ_c [106.2 (C-14)], and one olefinic quaternary carbon δ_c [153.4 (C-10)]. Based on ^{1}H-NMR, ^{13}C-NMR, and DEPT 135°, compound **1** has four unsaturated degrees. One unsaturation degree comes from the terminal olefinic group ($C=CH_2$), while the remaining comes from the tricyclic framework. The chemical shift from ^{1}H-NMR at δ_H 0.46 (1H, dd, *J* = 11.3, 9.5, 6.1 Hz, H-6) and 0.71 (1H, ddd, *J* =11.3, 9.4, 6.1 Hz, H-7), suggested the presence of a cyclopropane moiety of a sesquiterpenoid aromadendrane framework, and it was supported by the existence of an upfield quaternary carbon at δ_c 20.3 (C-11) [39]. Comparison of the NMR data of **1** with those of previously reported compounds revealed close agreement with spathulenol [40]. The optical rotation ($[\alpha]_D^{26}$ +1.25° (c 0.001, $CHCl_3$)) shows an agreement with (+)-spathulenol, confirming the stereochemistry of **1** [41].

Compound **2** was isolated as an epimeric mixture, which was obtained as a yellowish oil. On the basis of their ^{1}H-NMR and ^{13}C-NMR spectra, the ratio of mixture **2a** and **2b** was deduced as 4:1. Most of the signals were well-resolved for both compounds. Compound **2** yielded a molecular formula of $C_{15}H_{22}O_2$, as determined by HR-TOFMS, with an m/z value of 257.1520 $[M + Na]^+$ (calcd. 257.1517), indicating five unsaturation degrees. Furthermore, the ^{1}H-NMR spectra of the major compound **2a** presented one methyl singlet resonance at δ_H 1.32 (3H, s, CH_3-14) and two doublet methyl resonances at δ_H 0.94 (3H, d, CH_3-13), 0.93 (3H, d, CH_3-12). These methyls have the same *J* value, 6.8 Hz. Additionally, one methine sp^2 at δ_H 6.63 (1H, d, *J*=5.5 Hz, H-4) and an aldehyde proton resonance at δ_H 9.30 (1H, s, H-15) were also present in the ^{1}H-NMR spectrum. The ^{13}C-NMR spectrum accompanied by DEPT 135º of **2a** showed the presence of 15 carbons, including three methyls resonance at δ_c 19.7 (C-13), 22.0 (C-12), and 25.0 (C-14), four methylenes resonance at δ_c 38.9 (C-1), 19.7 (C-2), 26.8 (C-7), 35.2 (C-8), four methines at δ_c 53.2 (C5), 55.4 (C-6), 32.4 (C-11) including an olefinic methine at δ_c 158.7 (C-4), three quaternary carbons resonance at δ_c 59.7 (C-9), including an olefinic quaternary carbon resonance at δ_c 143.8 (C-3) and a carbonyl ketone at δ_c 212.2 (C-10), as well as one aldehyde at δ_c 192.8 (C-15). Based on ^{1}H-NMR, ^{13}C-NMR, and DEPT 135°, compound **2a** has a methine olefinic group (C=CH), a ketone, and an aldehyde. Therefore, the two remaining unsaturation degrees are attributed to the bicyclic system of a sesquiterpenoid. The presence of one quaternary aliphatic carbon, one tertiary methyl, and two secondary methyl carbons indicates the characteristic of isodaucane-type sesquiterpenoid [42]. The ^{1}H-NMR and ^{13}C-NMR resonances of **2a** and **2b** showed high similarity, supporting the same planar structure, with some chemical shift differences arising from stereochemical differences (Table 2). To further confirm the structure of this mixture, comprehensive 2D NMR experiments were performed (Figures S8–S11). ^{1}H-^{1}H COSY spectrum established the isodaucane skeleton, including the endocyclic double bond, as evidenced by the correlation between H-5 and the olefinic proton H-4. HMBC correlations were then used to assign the positions of the functional groups. The tertiary methyl at δ_H 1.32 (H-14) showed correlation with the quaternary carbon C-12 and the ketone at C-11, suggesting a neighboring position. In addition, the olefinic proton at δ_H 6.63 (H-4) showed correlation with the aldehyde (C-15), a methylene at C-2, and a quaternary at C-9. Based on these correlations, the planar structures of **2a** and **2b** were established, as shown in Figure 2. The NOESY experiment was conducted to further confirm the stereochemistry of both the major and minor components. H-14, a naturally occurring *β*-

 doi:10.20944/preprints202603.2471.v1

orientation proton in the isodaucane scaffold, was used as a reference to deduce the configurations of the remaining stereocenters [43,44]. In the major component **2a**, a NOESY correlation between H-14 and H-6 indicated a *β*-orientation for H-6. In contrast, compound **2b** showed NOESY correlations of H-14 with both H-6 and H-5, suggesting a difference at one stereogenic center and indicating that **2a** and **2b** constitute an epimeric mixture. Comparison of the NMR data of **2a** and **2b** with those of previously reported compounds revealed close agreement with 10-oxo-isodauc-3-en-15-al and sinulin A, respectively [43,45]. Accordingly, compounds **2a** and **2b** were identified as a mixture of 10-oxo-isodauc-3-en-15-al and sinulin A, isolated for the first time from *D. acutangulum* Miq.

Table 1. NMR data (700 MHz for ^{1}H and 175 MHz for ^{13}C, in $CDCl_3$) for **1**.

No of C	Compound **1**	
	δ_C (mult.)	δ_H ($\sum$H, m, *J* (Hz))
1	53.4 (d)	1.30 (1H, m)
2	26.7 (t)	1.91 (1H, qd, 11.7; 6.3) 1.63 (1H, m)
3	41.7 (t)	1.77 (1H, ddd, 12.8; 6.3; 1.5) 1.57 (1H, m)
4	81.0 (s)	-
5	54.3 (d)	1.31 (1H, m)
6	29.9 (d)	0.46 (1H, dd, 9.5; 11.3)
7	27.5 (d)	0.71 (1H, ddd, 11.3; 9.4; 6.1)
8	24.8 (t)	1.98 (1H, dtd, 14.3; 6.2; 1.7) 2.21 (1H, td, 10.5; 6.0)
9	38.8 (t)	2.42 (1H, dd, 6.3; 13.4) 2.04 (1H, t, 13)
10	153.4 (s)	-
11	20.3 (s)	-
12	16.3 (q)	1.04 (3H, s)
13	28.6 (q)	1.06 (3H, s)
14	106.2 (t)	4.66 (1H, br.s) 4.69 (1H, br.s)
15	26.1 (q)	1.28 (3H, s)

Table 2. NMR data (700 MHz for ^{1}H and 175 MHz for ^{13}C, in $CDCl_3$) for **2a** and **2b**.

No of C	Compound **2a**		Compound **2b**		HMBC
	δ_C (mult.)	δ_H ($\sum$H, m, *J* (Hz))	δ_C (mult.)	δ_H ($\sum$H, m, *J* (Hz))	
1	38.9 (t)	2.79 (1Ha, dt, 14.1, 5.3) 2.44 (1Hb, m)	38.0 (t)	2.56 (1H, m (overlap)) 2.43 (1H, m (overlap))	C2, C3, C10 C1, C3, C4, C10, C15
2	19.7 (t)	2.72 (1H, dt, 14.6, 5.2) 2.50 (1H, m)	20.1 (t)	3.00 (1H, ddd, 15.6, 7.1, 3.2) 2.05 (1H, m)	- C2, C1, C5, C9, C3, C15
3	143.8 (s)	-	143.7 (s)	-	C14, C6, C9, C3, C4, C10
4	158.7 (d)	6.63 (1H, d, 5.5)	157.5 (d)	6.78 (1H, 5.0, 2.0)	C13, C9, C5, C7
5	53.2 (d)	2.53 (1H, m)	49.1 (d)	2.48 (1H, m (overlap))	C5, C9, C6, C8
6	55.4 (d)	1.82 (1H, m)	49.4 (d)	2.08 (1H, m)	C14, C5, C9, C7
7	26.8 (t)	1.44 (1H, m) 1.86 (1H, m)	24.0 (t)	1.53 (1H, m) 1.91 (1H, m)	- -

 doi:10.20944/preprints202603.2471.v1

8	35.2 (t)	2.20 (1H, m) 1.41 (1H, m)	33.3 (t)	2.24 (1H, m) 1.57 (1H, m)	C7, C6 C6, C11, C13
9	59.7 (s)	-	60.3 (s)	-	C6, C11, C12
10	212.2 (s)	-	213.3 (s)	-	C8, C5, C9, C10
11	32.4 (d)	1.65 (1H, m)	31.5 (d)	1.67 (1H, m)	C2, C3, C4
12	22.0 (q)	0.93 (3H, d, 6.8)	21.6 (q)	0.93 (3H, d, 6.9)	C2, C3, C10
13	19.5 (q)	0.94 (3H, d, 6.8)	18.9 (q)	0.88 (3H, d, 6.7)	C1, C3, C4, C10, C15
14	25.0 (q)	1.32 (3H, s)	19.5 (q)	1.02 (3H, s)	-
15	192.8 (d)	9.34 (1H, s)	192.8 (d)	9.49 (1H, s)	C2, C1, C5, C9, C3, C15

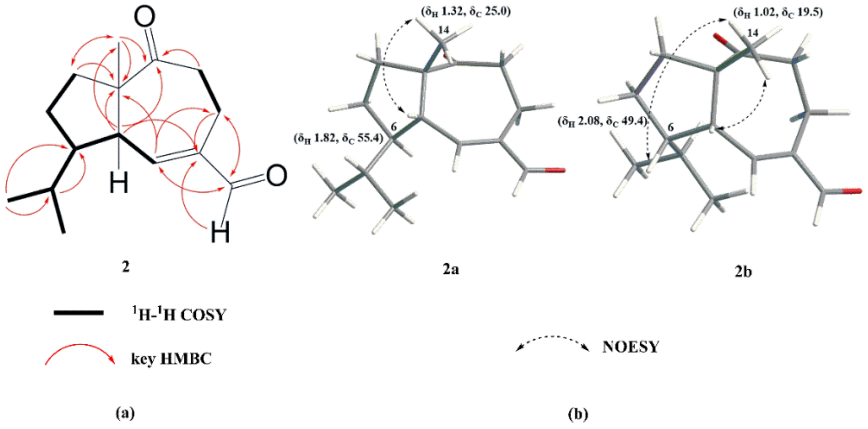

Figure 2. Selected ^{1}H-^{1}H COSY and HMBC correlations of **2** (a) and NOESY correlations of **2a** and **2b** (b).

Table 3 summarizes the antibiofilm activity of the *n*-hexane extract, isolated compounds **1** and **2**, and chlorhexidine against *Streptococcus mutans* ATCC 25175, expressed as minimum biofilm inhibitory concentration (MBIC). The *n*-hexane extract exhibited relatively weak activity, with an MBIC value of 2500 µg/mL. In contrast, the isolated compounds demonstrated markedly improved antibiofilm potency, where compounds **1** and **2** inhibited biofilm formation at 500 µg/mL and 250 µg/mL, respectively. Although chlorhexidine remained the most active reference agent (MBIC 62.5 µg/mL), the enhanced activity observed for the purified compounds compared to the crude extract clearly indicates that antibiofilm efficacy is concentrated within specific chemical constituents rather than the extract as a whole.

These findings underscore that a compound-oriented approach in the search for antibiofilm agents is more promising than relying on crude extracts. Isolation of single molecules not only enhances biological activity but also enables mechanistic elucidation at the molecular level, including target identification, binding interactions, and structure–activity relationship (SAR) analysis. Therefore, we conducted further investigations using in silico approaches to provide deeper insight into molecular interactions of sesquiterpenoid-based compounds with biofilm-associated targets and to rationalize their in vitro inhibitory profiles.

Table 3. Antibiofilm activity of compounds **1** and **2** against *S. mutans*.

Sample	MBIC (µg/mL)
	Streptococcus mutans ATCC 25175
n-hexane extract	2500
1	500
2	250
Chlorhexidine	62.5

 doi:10.20944/preprints202603.2471.v1

2.1. Molecular Docking Result

The molecular docking simulations provided significant insights into the binding preferences of the test ligands—**1**, **2a**, and **2b**—compared to the commercial antiseptic Chlorhexidine against three key virulence targets of *Streptococcus mutans*. The binding affinities and the nature of the chemical interactions are summarized in Table 4.

Across the receptors, chlorhexidine exhibited the strongest binding affinity for Sortase A (-7.931 kcal/mol) and GtfB (-8.309 kcal/mol). This suggests that while chlorhexidine is a potent general inhibitor compared to our ligand. The high stability of the chlorhexidine-GtfB complex can be attributed to a dense network of polar interactions, including conventional hydrogen bonds with residues such as Glu489, Asp562, and Asp567, supplemented by Pi-Pi stacked non-polar interactions as shown in Figure 4. In contrast, our ligands relied more heavily on a combination of non-polar interactions (Pi-alkyl/alkyl) and specific hydrogen bonding. For instance, in Sortase A (SrtA), as shown in Figure 3, ligand **2a** established polar interactions with Tyr241 and Thr167, which likely contribute to its superior affinity (-6.266 kcal/mol) compared to Spathulenol (-6.072 kcal/mol).

The computational analysis revealed that the test ligands exhibit moderate-to-high binding affinities toward the targeted *S. mutans* virulence proteins. Notably, the ligands demonstrated superior theoretical affinity for GtfC compared to the reference control, suggesting significant potential for disrupting the initial stages of biofilm scaffolding. These in silico observations provide a robust foundation for the subsequent in vitro MBIC evaluations (Table 3). The observed rank-order correlation validates the discriminatory power of the docking model, as it accurately categorized the potency profiles of the control and test compounds. Furthermore, the data align with the thermodynamic principles described by previously reported method [44], in which a ΔG variance of approximately 1.36 kcal/mol corresponds to a tenfold shift in binding magnitude. The transition from -8 to -6 kcal/mol represents a 20- to 30-fold difference in theoretical affinity, which is biologically consistent with the 4- to 8-fold increase observed in the experimental MBIC values in SrtA and GtfB enzymes.

Table 4. Molecular docking results targeted enzymes that contributed to biofilm production.

Receptors	Ligands	Binding affinity (kcal/mol)	Polar interaction (amino acid residue)	Non-polar interaction
Sortase A/SrtA (PDB ID: 4TQX)	**Chlorhexidine**	**-7.931**	Phe237[a], Gln239[a], Tyr241[ac], Gln243[a], Phe246[ac]	Pi-alky/alkyl
	1	-6.072	-	Pi-alkyl/alkyl
	2a	-6.266	Tyr241[a], Thr167[b]	Pi-alkyl/alkyl
	2b	-6.072	Arg238[b]	Pi-alkyl/alkyl
Glucosyltransferase B/GtfB (PDB ID: 8FK4)	**Chlorhexidine**	**-8.309**	Glu489[ac], Asp562[ac], Asp567[ac], Tyr584[ac], Tyr404[b]	Pi-alkyl, Pi-Pi stacked
	1	-7.166	Glu489[a]	Pi-alkyl/alkyl
	2a	-7.001	Asn888[a], Gln566[b]	-
	2b	-6.949	Trp491[a]	-

a: conventional hydrogen bond. b: carbon-hydrogen bond. c: attractive charge/Pi-cation.

 doi:10.20944/preprints202603.2471.v1

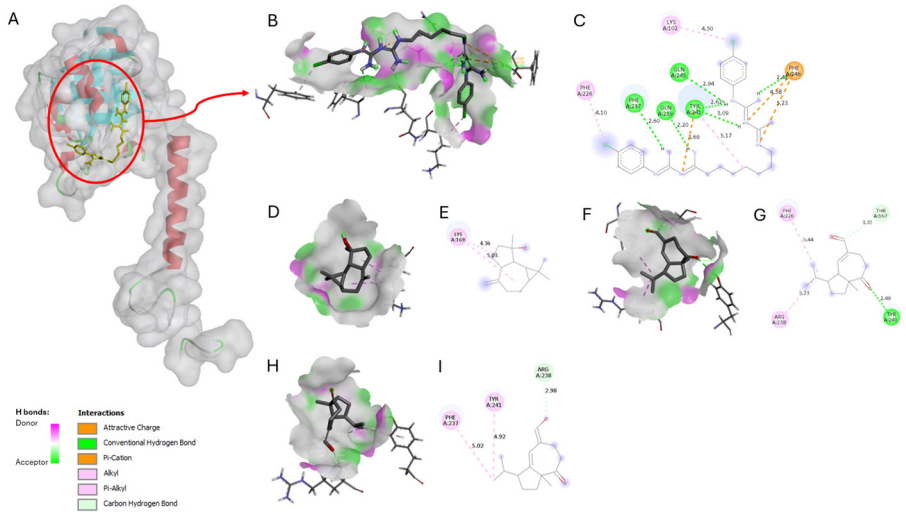

Figure 3. Molecular docking analysis showing the 3D binding modes and 2D interaction profiles of Chlorhexidine and the isolated compounds (**1**, **2a**, and **2b**) within the active site of *Streptococcus mutans* Sortase A (SrtA). (A) Full view of the Sortase A protein surface and binding pocket indicated by red circle; (B) Close-up 3D view of Chlorhexidine in the binding site; (C) 2D interaction diagram for Chlorhexidine; (D, F, H) 3D binding poses of **1**, **2a**, and **2b**; (E, G, I) Corresponding 2D interaction maps for the ligands in D, F, and H.

In line with the previous bioassay evaluation of the three isolated sesquiterpenoids (compounds **1**, **2a**, and **2b**), the concordance between the in silico docking data (Table 4) and the in vitro MBIC results (Table 3) further reinforces the predictive validity of the computational model. Although compound **1** theoretically displayed comparable or slightly favorable binding energies toward SrtA and GtfB relative to **2b** (−6.072 vs −6.072 kcal/mol in SrtA; −7.166 vs −6.949 kcal/mol in GtfB), its in vitro antibiofilm activity (MBIC 500 µg/mL) was inferior to compound **2** (MBIC 250 µg/mL). This apparent discrepancy can be rationalized by hypothesizing a cooperative or multi-target effect between isomeric constituents **2a** and **2b** within compound **2**, leading to enhanced biological efficacy compared to a single sesquiterpenoid entity.

Such synergistic or sensitization phenomena have been widely reported for sesquiterpenes; for instance, nerolidol mixtures (including cis-, trans-, and racemic forms) has been reported to potentiate the antibacterial efficacy of multiple antibiotics against *Staphylococcus aureus* and *Escherichia coli*, resulting in significantly reduced MIC values through membrane-disruptive and permeability-enhancing mechanisms [47–49]. The combined presence of **2a** and **2b** may facilitate improved target accessibility, membrane interaction, or multi-site engagement within *S. mutans* virulence enzymes, thereby amplifying antibiofilm performance beyond what is predicted solely from individual docking scores. Therefore, while docking accurately discriminated the general potency hierarchy (chlorhexidine > test ligands), the biological outcome underscores the importance of compositional and cooperative effects in sesquiterpenoid-based antibiofilm agents. Collectively, these findings not only demonstrate alignment between thermodynamic predictions and experimental MBIC trends but also provide new insight into the potential of sesquiterpenoid mixtures as promising antibiofilm scaffolds, warranting further mechanistic and combination-based investigations.

 doi:10.20944/preprints202603.2471.v1

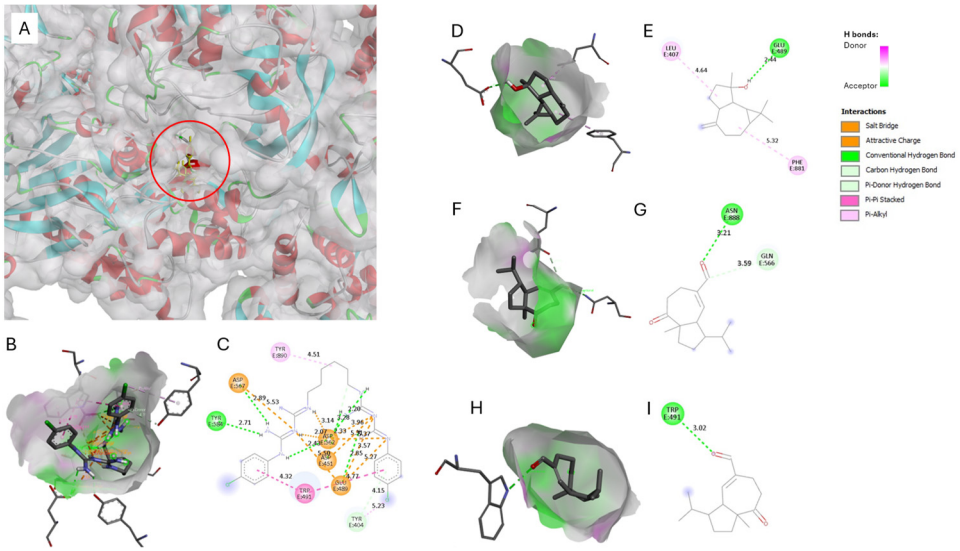

Figure 4. Molecular docking analysis showing the 3D binding modes and 2D interaction profiles of Chlorhexidine and the isolated compounds (**1**, **2a**, and **2b**) within the active site of *Streptococcus mutans* GtfB. (A) View of binding pocket of GtfB indicated by red cirlce; (B) Close-up 3D view of Chlorhexidine in the binding site; (C) 2D interaction diagram for Chlorhexidine; (D, F, H) 3D binding poses of **1**, **2a**, and **2b**; (E, G, I) Corresponding 2D interaction maps for the ligands in D, F, and H.

3. Materials and Methods

3.1. General Experimental Prosedures

Infrared spectra were measured on a Perkin-Elmer Spectrum 100 with KBr disk (Waltham, Massachusetts, USA). Mass spectra were measured with a waters XEVO HR-TOF-ESI-MS (Milford, MA) complemented with ESI+ mode. The NMR spectra were recorded with internal standard as a TMS on a Bruker Ascend spectrometer, involving ^{1}H at 700 MHz, ^{13}C at 175 MHz, DEPT 135°, ^{1}H-^{1}H COSY, HMBC, HSQC, and NOESY. Vacuum liquid chromatography (VLC) and column chromatography (CC) were performed on silica gel 60 (Merck KGaA, Darmstadt, Germany, 70–230 and 230–400 mesh) and octadecyl silane (ODS, Chromatorex C18 DM1020T, Fuji Sylisia Chemical Ltd., Japan, 100–200 mesh). The isolation guidance was utilized in a thin layer chromatography (TLC) using silica gel 60 F_{254} (Merck KGaA, Darmstadt, Germany) plates of the normal phase and the reverse one using reverse phase RP-18 F_{254S} plates (Merck KGaA, Darmstadt, Germany). Detection of the TLC plate was monitored under UV light at 254 and 365 nm before spraying with 10% H_2SO_4 in ethanol, followed by heating. The bacterial strain used for antibiofilm activity evaluation was *Streptococcus mutans* ATCC 25175.

3.2. Plant Material

The sample was *D. acutangulum* Miq. twigs which were gained from Bogor Botanical Garden, Bogor, West Java Province, Indonesia. The sample was determined with number of specimen (III.F.20) at Herbarium Bogoriense, West Java Province, Indonesia.

3.3. Extraction and Isolation

Dried twig powder of *D. acutangulum* Miq. (5.6 kg) was macerated with 96% ethanol at room temperature. The resulting macerate was filtered and concentrated under reduced pressure using a rotary evaporator at 40 °C to afford a crude ethanolic extract (340.9 g). The crude extract was subsequently suspended and subjected to successive liquid–liquid partitioning based on solvent polarity using *n*-hexane, ethyl acetate, and *n*-butanol. Each fraction was concentrated under vacuum to yield *n*-hexane extract (37.5 g), ethyl acetate extract (113 g), and *n*-butanol extract (1 g), respectively.

 doi:10.20944/preprints202603.2471.v1

The *n*-hexane extract (37.5 g) was separated on vacuum liquid chromatography (VLC) with a stepwise gradient of *n*-hexane: EtOAc: MeOH (100:0-0:100-100:0, 10% v/v) to yield 11 fractions (Fr. A - K). Fr. C (6.3 g) was chromatographed on silica gel CC using a stepwise gradient of *n*-hexane:EtOAc (100:0-0:100, 1% v/v) to yield 10 subfractions (Fr. C – C10). Fr. C6 (306 mg) was subjected to ODS CC using MeOH:H_2O (8:2) to yield 7 subfractions (Fr. C6.1 – C6.7). Fr. C6.5 (16 mg) was subjected to CC silica gel with *n*-hexane:DCM (6:4) to afford **1** (10 mg). Fr. C8 (638 mg) was subjected to CC silica gel with *n*-hexane:DCM (5:5) to yield 4 subfractions (Fr. C8.1 – C8.4). Subsequently, Fr. C8.3 (45 mg) was subjected to ODS CC using MeOH:H_2O (6:4) to afford an epimeric mixture of **2a** and **2b** (7 mg).

Spathulenol (**1**): Colorless oil, IR (KBr) ν_{max} cm^{-1}: 3388; 2928; 1635; 1454; 1375; 1128 cm^{-1}; ^{1}H-NMR ($CDCl_3$, 700 MHz); ^{13}C-NMR ($CDCl_3$, 175 MHz), see Table 1; HR-TOFMS m/z 221.1910 $[M+H]^+$ (calculated for $C_{15}H_{24}O$, m/z 221.1905).

10-oxo-isodauc-3-en-15-al (**2a**) and sinulin A (**2b**): Yellowish oil; ^{1}H-NMR ($CDCl_3$, 700 MHz); ^{13}C-NMR ($CDCl_3$, 175 MHz), see Table 2; HR-TOFMS m/z 257.1520 $[M+Na]^+$ (calculated for $C_{15}H_{22}O_2Na$, m/z 257.1517).

3.4. Determination of Antibiofilm Activity

The antibiofilm activity was evaluated by determining the Minimum Biofilm Inhibitory Concentration (MBIC) using a crystal violet microdilution assay in a 96-well microplate. All equipment and materials were sterilized by autoclaving at 121 °C for 15 min prior to use. The test bacteria were grown on agar media at 37 °C for 18–24 h, and several colonies were suspended in Brain Heart Infusion Broth (BHIB) supplemented with 2% sucrose and incubated for a further 18–24 h. The bacterial suspension was adjusted to 0.5 McFarland standard (≈1–2 × 10^8 CFU/mL) and dispensed into the microplate with appropriate controls, including sample control, negative control, solvent control, and positive control (chlorhexidine). After adding test samples and performing serial dilutions, the plate was incubated for 18–48 h. The wells were then washed with PBS, stained with 1% crystal violet, and the bound dye was solubilized with 30% glacial acetic acid. Biofilm formation was quantified by measuring absorbance at 595 nm using a multimode microplate reader.

3.5. Molecular Docking Analysis

Molecular docking analysis was run for understanding the theoretical interaction between compounds 1 and 2 and the enzymes in *S. mutans*. The biofilm formation in *S. mutans* is produced because of the activity of Sortase A (SrtA) and Glucotransferases (Gtfs), including GtfB, GtfC, and GtfD [36—38]. The three-dimensional structures of all target protein structures for SrtA (4TQX) and GtfB (8FK4) were obtained from the RCSB Protein Data Bank. Protein preparation involved removing water molecules, adding polar hydrogens, and assigning Kollman charges using AutoDockTools within a Python environment in Jupyter Notebook. Molecular docking was executed using AutoDock Vina. As we did blind docking, we created tiled grid box for finding the binding site throughout the protein structure. The grid box searched for each protein described as follows, 4TQX coordinate at 18.0Å, 24.0Å, -3.0Å, and size at 40Å, 51Å, 70Å; 8FK4 coordinate at 24.0Å, 33.0Å, 118.0Å, and size at 70Å, 73Å, 118Å. Then, after tiling the grid box, the grid coordinate that produced highest binding affinity has chosen as follows, 4TQX coordinate at 23.0Å, 34.5Å, -8.0Å, and size at 30Å, 30Å, 30Å; 8FK4 coordinate at 44.0Å, 54.5Å, 74.0Å, and size at 30Å, 30Å, 30Å. The docking results were ranked based on the binding affinity scores (kcal/mol), and the binding interactions were visualized in BIOVIA Discovery Studio.

4. Conclusions

In conclusion, this study successfully isolated sesqiterpenoids for the first time from the *n*-hexane extract of *D. acutangulum* Miq. twigs. The identified compounds, spathulenol (**1**), along with 10-oxo-isodauc-3-en-15-al (**2a**) and sinulin A (**2b**) as an epimeric mixture, are noteworthy, particularly for the novelty of compounds **1** and **2** within this genus. In vitro evaluation against *Streptococcus*

 doi:10.20944/preprints202603.2471.v1

mutans demonstrated weak antibiofilm activity (MBIC 250–500 μg/mL), which remains lower than that of chlorhexidine as the reference control.

The in silico analysis supported the experimental findings by revealing similarly moderate binding affinities toward Sortase A and GtfB, with a consistent rank-order trend. The relatively better activity observed for the epimeric mixture compared to the single compound suggests a possible additive or multicomponent contribution under biological conditions. Overall, this study provides an initial structure–activity relationship insight into sesquiterpenoids as antibiofilm candidates, although further optimization and mechanistic investigations are required to enhance their therapeutic relevance.

Supplementary Materials: The following supporting information can be downloaded at the website of this paper posted on Preprints.org, Figure S1: HRTOFMS Spectrum of **1**; Figure S2: FTIR Spectrum of **1**; Figure S3: ^{1}H-NMR Spectrum of **1**; Figure S4: ^{13}C-NMR and DEPT-135° Spectrum of **1**; Figure S5: HRTOFMS Spectrum of **2**; Figure S6: ^{1}H-NMR Spectrum of **2**; Figure S7: ^{13}C-NMR and DEPT-135° Spectrum of **2**; Figure S8: HSQC Spectrum of **2**; Figure S9: ^{1}H-^{1}H-COSY Spectrum of **2**; Figure S10: HMBC Spectrum of **2**; Figure S11. NOESY Spectrum of **2**.

Author Contributions: Conceptualization, R.A. and U.S.; methodology, A.A.N., K.F., and U.S.; investigation, R.A., H.A., and C.N.U.I.; software, E.E.P. and A.N.; data curation, R.A., H.A., C.N.U.I., A.A.N., and K.F.; validation, A.A.N. and E.J.; formal analysis, R.A., E.E.P., and A.N.; resources, U.S.; visualization, E.J. and E.E.P.; supervision, U.S.; writing—original draft preparation, H.A., C.N.U.I., and E.J.; writing—review and editing, R.A., A.A.N., and K.F.; project administration, R.A. and U.S.; funding acquisition, R.A. All authors have read and agreed to the published version of the manuscript.

Funding: This research was funded by Universitas Padjadjaran, Indonesia, through the Academic Leadership Grant (No. 1630/UN6.3.1/PT.00/2024). The authors also acknowledge the Advanced Chemical Characterization Laboratory, BRIN, for providing facilities and scientific and technical support through E-Layanan Sains – BRIN.

Institutional Review Board Statement: Not applicable.

Informed Consent Statement: Not applicable.

Data Availability Statement: Not applicable.

Acknowledgments: The authors acknowledge the Advanced Chemical Characterization Laboratory, National Research and Innovation Agency (BRIN), for providing facilities as well as scientific and technical support through E-Layanan Sains – BRIN during this study.

Conflicts of Interest: The authors declare no conflict of interest.

References

1. Celik, K.; Togar, B.; Turkez, H.; Taspinar, N. In vitro cytotoxic, genotoxic, and oxidative effects of acyclic sesquiterpene farnesene. *Turk. J. Biol.* **2014**, *38*, 253–259. https://doi.org/10.3906/biy-1309-55
2. Buckle, J. *Clinical Aromatherapy: Essential Oil in Practice*, 3rd ed.; Elsevier Health Sciences: London, UK, 2015; pp. 45–46.
3. Li, X.; Zhang, M.; Liu, Y.; Feng, Y.; Yang, J.; Xie, Y.; Li, Y.; Xu, Y.; Huang, Z. Recent advances in the development of bergamot (*Citrus bergamia* Risso) essential oil: From extraction, chemical composition, function to potential applications. *Ind. Crops Prod.* **2026**, *240*, 122617. https://doi.org/10.1016/j.indcrop.2025.122617
4. Zheng, Q.; Zhu, H.; Yang, H.P.; Peng, C.; Wu, G.X.; Zhou, Q.M.; Xiong, L. Guaiane-type sesquiterpenoids from patchouli oil and their potential anti-depressive effects. *Phytochemistry* **2025**, *243*, 114738. https://doi.org/10.1016/j.phytochem.2025.114738
5. Lin, S.H.; Diao, N.; Wang, Y.; Liang, D. Structurally diverse sesquiterpenoid glycosides with anti-inflammatory activity from *Cissampelopsis spelaeicola*. *Phytochemistry* **2025**, *243*, 114734. https://doi.org/10.1016/j.phytochem.2025.114734

 doi:10.20944/preprints202603.2471.v1

6. Li, B.; Zhou, S.; Wu, W.; Tian, Y.; Ren, Y.; Ma, J.; Zang, Y.; Yuan, Y.; Zhang, D.; Li, C. Atractylodimers A–D, unprecedented sesquiterpenoid dimers with cage-like skeletons from *Atractylodes macrocephala* and their neuroprotective activities. *Chin. J. Nat. Med.* **2025**, *23*, 100010. https://doi.org/10.1016/j.cjnm.2025.100010
7. Zhang, F.Y.; Gan, L.; Hu, X.Y.; Zhu, G.H.; Liao, Y.L.; Huang, G.S.; Guo, D.; Li, W. Saglabranoids A–J, structurally diverse sesquiterpenoids with anti-hepatic fibrosis activity from the roots of *Sarcandra glabra*. *J. Mol. Struct.* **2026**, *1357*, 145333. https://doi.org/10.1016/j.molstruc.2026.145333
8. Wang, M.; Zhao, L.; Chen, K.; Shang, Y.; Wu, J.; Guo, X.; Chen, Y.; Liu, H.; Tan, H.; Qiu, S.X. Antibacterial sesquiterpenes from the stems and roots of *Thuja sutchuenensis*. *Bioorg. Chem.* **2020**, *96*, 103645. https://doi.org/10.1016/j.bioorg.2020.103645
9. Wang, Z.X.; Kong, W.Z.; Guan, S.N.; Zhang, N.; Yu, Y.B.; Zhang, X.Y. Pitsubcosides M–S: Novel antibacterial cadinane sesquiterpenoid glycoside esters from *Pittosporum subulisepalum*. *Ind. Crops Prod.* **2024**, *208*, 117917. https://doi.org/10.1016/j.indcrop.2023.117917
10. Vestby, L.K.; Grønseth, T.; Simm, R.; Nesse, L.L. Bacterial biofilm and its role in the pathogenesis of disease. *Antibiotics* **2020**, *9*, 59. https://doi.org/10.3390/antibiotics9020059
11. Perry, E.K.; Tan, M.W. Bacterial biofilms in the human body: Prevalence and impacts on health and disease. *Front. Cell. Infect. Microbiol.* **2023**, *13*, 1237164. https://doi.org/10.3389/fcimb.2023.1237164
12. Matsumoto-Nakano, M. Role of *Streptococcus mutans* surface proteins for biofilm formation. *Jpn. Dent. Sci. Rev.* **2018**, *54*, 22–29.
13. Khushbu, Y.; Satyam, P. Dental caries: A review. *Asian J. Biomed. Pharm. Sci.* **2016**, *6*, 1–7. https://doi.org/10.1016/j.jdsr.2017.08.002
14. Riyadi, S.A.; Naini, A.A.; Supratman, U. Sesquiterpenoids from Meliaceae family and their biological activities. *Molecules* **2023**, *28*, 4874. https://doi.org/10.3390/molecules28124874
15. Izdihar, G.; Naini, A.A.; Harneti, D.; Maharani, R.; Nurlelasari, N.; Safari, A.; Farabi, K.; Supratman, U.; Azmi, M.N. Sesquiterpenoids from the stem bark of *Aglaia simplicifolia* and their cytotoxic activity against B16-F10 melanoma skin cancer cell. *Indones. J. Chem.* **2021**, *21*, 1560–1567. https://doi.org/10.22146/ijc.68383
16. Naini, A.A.; Mayanti, T.; Supratman, U. Triterpenoids from *Dysoxylum* genus and their biological activities. *Arch. Pharm. Res.* **2022**, *45*, 63–89. https://doi.org/10.1007/s12272-022-01371-9
17. Parulian, S.S.; Nurlelasari, N.; Naini, A.A.; Hilmayanti, E.; Mayanti, T.; Harneti, D.; Darwati, D.; Maharani, R.; Farabi, K.; Supratman, U.; Anwar, R.; Fajriah, S.; Azmi, M.N.; Shiono, Y. Sesquiterpenoids from stem bark of *Chisocheton lasiocarpus* and their cytotoxic activity against MCF-7 breast cancer cell. *Molekul* **2022**, *17*, 413–420. https://doi.org/10.20884/1.jm.2022.17.3.6425
18. Kouame, C.; Ouattara, Z.A.; Kambire, D.A.; Monteil, M.; Mamyrbekova, J.A.; Bighelli, A.; Tomi, F.; Lecouvey, M.; Bekro, Y.A. Chemical composition and biological activity of *Guarea cedrata* leaf and root bark essential oil. *Int. J. Biochem. Res. Rev.* **2022**, *31*, 27–35. 10.9734/IJBCRR/2022/v31i9779
19. Adeniyi, B.A.; Adagbasa, O.O.; Idowu, P.A.; Igbokwe, C.O.; Moody, J.O.; Aiyelaagbe, O.O. Extracts of *Trichilia heudelotii* (Meliaceae), a Nigerian medicinal plant, have antibacterial and antifungal activity. *J. Pharm. Res. Int.* **2024**, *36*, 24–33. 10.9734/jpri/2024/v36i37504
20. Fadhilah, K.; Wahyuono, S.; Astuti, P. A. Sesquiterpene aldehyde isolated from ethyl acetate extract of *Lansium domesticum* fruit peel. *Indones. J. Pharm.* **2021**, *32*, 394–398. https://doi.org/10.22146/ijp.1884
21. Nugroho, A.E.; Sugiura, R.; Momota, T.; Hirasawa, Y.; Wong, C.P.; Kaneda, T.; Hadi, A.H.A.; Morita, H. Dysosesquiflorins A and B, sesquiterpenoids from *Dysoxylum densiflorum*. *J. Nat. Med.* **2015**, *69*, 411–415. 10.1007/s11418-015-0888-6
22. Naini, A.A.; Mayanti, T.; Nurlelasari; Harneti, D.; Maharani, R.; Safari, A.; Hidayat, A.C.; Farabi, K.; Lesmana, R.; Supratman, U.; Shiono, Y. Cytotoxic sesquiterpenoids from *Dysoxylum parasiticum* (Osbeck) Kosterm. stem bark. *Phytochem. Lett.* **2022**, *47*, 102-106. https://doi.org/10.1016/j.phytol.2021.11.010
23. Naini, A.A.; Mayanti, T.; Harneti, D.; Darwati, D.; Nurlelasari, N.; Maharani, R.; Farabi, K.; Herlina, T.; Supratman, U.; Fajriah, S.; Kuncoro, H.; Azmi, M.N.; Shiono, Y.; Jungsuttiwong, S.; Chakthong, S. Sesquiterpenoids and sesquiterpenoid dimers from the stem bark of *Dysoxylum parasiticum*. *Phytochemistry* **2023**, *205*, 113477. https://doi.org/10.1016/j.phytochem.2022.113477
24. Gu, J.; Cheng, G.G.; Qian, S.Y.; Li, Y.; Liu, Y.P.; Luo, X.D. Dysoxydensins A–G, seven new clerodane diterpenoids from *Dysoxylum densiflorum*. *Planta Med.* **2014**, *80*, 1017–1022. 10.1055/s-0034-1382903

 doi:10.20944/preprints202603.2471.v1

25. Zhang, P.Z.; Zhang, Y.M.; Lin, Y.; Wang, F.; Zhang, G.L. Three new diterpenes from *Dysoxylum lukii* and their NO production inhibitory activity. *J. Asian Nat. Prod. Res.* **2020**, *22*, 531–536. 10.1080/10286020.2019.1607839
26. Ragasa, C.Y.; Torres, O.B.; Bernardo, L.O.; Mandia, E.H.; Don, M.J.; Shen, C.C. Glabretal-type triterpenoids from *Dysoxylum mollissimum*. *Phytochem. Lett.* **2013**, *6*, 514–518. https://doi.org/10.1016/j.phytol.2013.06.010
27. He, X.F.; Wang, X.N.; Yin, S.; Dong, L.; Yue, J.M. Ring A-seco triterpenoids with antibacterial activity from *Dysoxylum hainanense*. *Bioorg. Med. Chem. Lett.* **2011**, *21*, 125–129. https://doi.org/10.1016/j.bmcl.2010.11.057
28. Bhardwaj, N.; Gupta, P.; Tripathi, N.; Chakrabarty, S.; Verma, A.; Kumari, S.; Gautam, V.; Ravikanth, G.; Jain, S.K. New ring-A modified cycloartane triterpenoids from *Dysoxylum malabaricum* bark: Isolation, structure elucidation and cytotoxicity. *Steroids* **2024**, *205*, 109390. https://doi.org/10.1016/j.steroids.2024.109390
29. Yan, H.J.; Wang, J.S.; Kong, L.Y. Cytotoxic dammarane-type triterpenoids from the stem bark of *Dysoxylum binecteriferum*. *J. Nat. Prod.* **2014**, *77*, 234–242. https://doi.org/10.1021/np400700g
30. Riyadi, S.A.; Naini, A.A.; Mayanti, T.; Lesmana, R.; Azmi, M.R.; Fajriah, S.; Jungsuttiwong, S.; Supratman, U. Alliaxylines A–E: Five new mexicanolides from the stem bark of *Dysoxylum alliaceum*. *J. Nat. Med.* **2024**, *78*, 558–567. https://doi.org/10.1007/s11418-024-01794-2
31. Xu, J.; Ni, G.; Yang, S.; Yue, J. Dysoxylumasins A–F: Six new limonoids from *Dysoxylum mollissimum*. *Chin. J. Chem.* **2013**, *31*, 72–78. https://doi.org/10.1002/cjoc.201200838
32. Liu, W.X.; Tang, G.H.; He, H.P.; Zhang, Y.; Li, S.L.; Hao, X.J. Limonoids and triterpenoids from the twigs and leaves of *Dysoxylum hainanense*. *Nat. Prod. Bioprospect.* **2012**, *2*, 29–34. 10.1007/s13659-011-0030-8
33. Naini, A.A.; Mayanti, T.; Maharani, R.; Harneti, D.; Nurlelasari, N.; Farabi, K.; Fajriah, S.; Hilmayanti, E.; Kabayama, K.; Shimoyama, A.; Manabe, Y.; Fukase, K.; Jungsuttiwong, S.; Prescott, T.A.K.; Supratman, U. Paraxylines A–G: Highly oxygenated preurianin-type limonoids with immunomodulatory TLR4 and cytotoxic activities from the stem bark of *Dysoxylum parasiticum*. *Phytochemistry* **2024**, *220*, 114009. 10.1016/j.phytochem.2024.114009
34. Riyadi, S.A.; Naini, A.A.; Mayanti, T.; Farabi, K.; Harneti, D.; Nurlelasari, N.; Maharani, R.; Lesmana, R.; Fajriah, S.; Jungsuttiwong, S.; Awang, K.; Azmi, M.N.; Supratman, U. Alliaceumolide A: A rare undescribed 17-membered macrolide from Indonesian *Dysoxylum alliaceum*. *Phytochem. Lett.* **2024**, *62*, 73–77. https://doi.org/10.1016/j.phytol.2024.07.004
35. Dharmayani, N.K.T.; Yoshimura, T.; Hermawati, E.; Juliawaty, L.D.; Syah, Y.M. Antibacterial and antifungal two phenolic sesquiterpenes from *Dysoxylum densiflorum*. *Z. Naturforsch. C* **2020**, *75*, 1–5. https://doi.org/10.1515/znc-2019-0072
36. Cho, E.; Hwang, J.Y.; Park, J.S.; Oh, D.; Oh, D.C.; Park, H.G.; Shin, J.; Oh, K.B. Inhibition of *Streptococcus mutans* adhesion and biofilm formation with small-molecule inhibitors of sortase A from *Juniperus chinensis*. *J. Oral Microbiol.* **2022**, *14*, 2088937. 10.1080/20002297.2022.2088937
37. Nijampatnam, B.; Ahirwar, P.; Pukkanasut, P.; Womack, H.; Casals, L.; Zhang, H.; Cai, X.; Michalek, S.M.; Wu, H.; Velu, S.E. Discovery of potent inhibitors of *Streptococcus mutans* biofilm with antivirulence activity. *ACS Med. Chem. Lett.* **2020**, *12*, 48–55. 10.1021/acsmedchemlett.0c00373
38. Ren, Z.; Cui, T.; Zeng, J.; Chen, L.; Zhang, W.; Xu, X.; Cheng, L.; Li, M.; Li, J.; Zhou, X.; Li, Y. Molecule targeting glucosyltransferase inhibits *Streptococcus mutans* biofilm formation and virulence. *Antimicrob. Agents Chemother.* **2016**, *60*, 126–135. 10.1128/AAC.00919-15
39. Feliciano, A.S.; Medarde, M.; Gordaliza, M.; Del Olmo, E.; Miguel del Corral, J.M. Sesquiterpenoids and phenolics of *Pulicaria paludosa*. *Phytochemistry* **1989**, *28*, 2717–2721. https://doi.org/10.1016/S0031-9422(00)98074-9
40. Gunawan, L.; Mustofa, H.N.; Naini, A.A.; Harneti, D.; Hidayat, A.T.; Nurlelasari, N.; Maharani, R.; Mayanti, T.; Fajriah, S.; Awang, K.; Azmi, M.N.; Supratman, U. Sesquiterpenoids from *Dysoxylum amooroides* stem bark: Isolation, structure determination, and cytotoxicity against MCF-7 breast cancer cells. *Indones. J. Chem.* **2025**, *25*, 157–168. 10.22146/ijc.99121
41. Aguilar-Guadarrama, A.B.; Rios, M.Y. Three new sesquiterpenes from *Croton arboreous*. *J. Nat. Prod.* **2004**, *67*, 914–917. https://doi.org/10.1021/np030485f

 doi:10.20944/preprints202603.2471.v1

42. Jares, E.A.; Potolovskii, L.A.; Katrenko, T.I.; Polyakova, A.A.; Fufaev, A.A.; Bessonova, R.N.; Terweij-Groen, C.P.; Heemstra, S.; Kraak, J.C. Isolation of sesquiterpenes from *Senecio crassiflorus* by combined dry column and high performance liquid chromatography. *J. High Resolut. Chromatogr.* **1989**, *12*, 565–568. **https://doi.org/10.1002/jhrc.1240120821**
43. Misra, L.N.; Jakupovic, J.; Bohlmann, F.; Schmeda-Hirschmann, G. Isodaucane derivatives, norsesquiterpenes and clerodanes from *Chromolaena laevigata*. *Tetrahedron* **1985**, *41*, 5353–5356. https://doi.org/10.1016/S0040-4020(01)96789-4
44. Bülow, N.; König, W.A. The role of germacrene D as a precursor in sesquiterpene biosynthesis: Investigations of acid-catalyzed, photochemical and thermally induced rearrangements. *Phytochemistry* **2000**, *55*, 141–168. https://doi.org/10.1016/S0031-9422(00)00266-1
45. Qin, G.F.; Tang, X.L.; Sun, Y.T.; Luo, X.C.; Zhang, J.; Ofwegen, L.V.; Sung, P.J.; Li, P.L.; Li, G.Q. Terpenoids from the soft coral *Sinularia* sp. collected in Yongxing Island. *Mar. Drugs* **2018**, *16*, 127. https://doi.org/10.3390/md16040127
46. Welsch, M.E.; Kaplan, A.; Chambers, J.M.; Stokes, M.E.; Bos, P.H.; Zask, A.; Zhang, Y.; Sanchez-Martin, M.; Badgley, M.A.; Huang, C.S.; Tran, T.H.; Akkiraju, H.; Brown, L.M.; Nandakumar, R.; Cremers, S.; Yang, W.S.; Tong, L.; Olive, K.P.; Ferrando, A.; Stockwell, B.R. Multivalent small-molecule pan-RAS inhibitors. *Cell* **2017**, *168*, 878–889. 10.1016/j.cell.2017.02.006
47. Gonçalves, O.; Pereira, R.; Gonçalves, F.; Mendo, S.; Coimbra, M.A.; Rocha, S.M. Evaluation of the mutagenicity of sesquiterpenic compounds and their influence on the susceptibility towards antibiotics of two clinically relevant bacterial strains. *Mutat. Res. Genet. Toxicol. Environ.* **2011**, *723*, 18–25. https://doi.org/10.1016/j.mrgentox.2011.03.010
48. Simões, M.; Rocha, S.; Coimbra, M.A.; Vieira, M.J. Enhancement of *Escherichia coli* and *Staphylococcus aureus* antibiotic susceptibility using sesquiterpenoids. *Med. Chem.* **2008**, *4*, 616–623. https://doi.org/10.2174/157340608786242016
49. Curvelo, J.A.R.; Marques, A.M.; Barreto, A.L.S.; Romanos, M.T.V.; Portela, M.B.; Kaplan, M.A.C.; Soares, R.M.A. A novel nerolidol-rich essential oil from *Piper claussenianum* modulates *Candida albicans* biofilm. *J. Med. Microbiol.* **2014**, *63*, 697–702. 10.1099/jmm.0.063834-0